Fr-HMGB1 and ds-HMGB1 activate the kynurenine pathway via different mechanisms in association with depressive-like behavior

BO WANG[1], YONG-JIE LIAN[1,2], WEN-JUN SU[1], LIN-LIN LIU[1,3], JIA-MEI LI[1], CHUN-LEI JIANG[1] and YUN-XIA WANG[1]

[1]Laboratory of Stress Medicine, Department of Psychology and Mental Health; [2]Department of Neurology, Changhai Hospital, Second Military Medical University, Shanghai 200433; [3]Department of Nursing, The 474th Hospital of The People's Liberation Army, Urumqi, Xinjiang 830012, P.R. China

Received October 12, 2018; Accepted April 25, 2019

DOI: 10.3892/mmr.2019.10225

Abstract. Our previous study reported that fully reduced high mobility group box 1 (fr-HMGB1) and disulfide HMGB1 (ds-HMGB1) induce depressive-like behavior; however, the underlying mechanisms remain unclear. In the present study, the induction of depression via the kynurenine pathway by different redox states of HMGB1 was investigated *in vivo* and *in vitro*. To evaluate the expression of enzymes of the kynurenine pathway, reverse transcription-quantitative PCR and western blot analyses were conducted. Additionally, cytokine levels were measured by ELISAs. Following intracerebroventricular injection of ds- and fr-HMGB1, behavioral tests were performed, revealing the presentation of depressive-like behavior, and essential proteins in the kynurenine pathway were demonstrated to be upregulated at the mRNA level, suggesting that ds- and fr-HMGB1 contributed to the development of this behavior via the kynurenine pathway. ds-HMGB1 directly activated the kynurenine pathway and cytokines such as tumor necrosis factor-α (TNF-α) and interleukin-1β (IL-1β) in the hippocampal tissue. Conversely, fr-HMGB1 upregulated the aforementioned factors only following treatment with H_2O_2. These findings indicated that ds-HMGB1 induced depression in a manner associated with the kynurenine pathway, whereas oxidation of fr-HMGB1 evoked activation of the kynurenine pathway, resulting in depressive behavior.

Correspondence to: Professor Yun-Xia Wang, Laboratory of Stress Medicine, Department of Psychology and Mental Health, Second Military Medical University, 800 Xiangyin Road, Shanghai 200433, P.R. China
E-mail: cloudywang66@163.com

Key words: fully reduced high mobility group box 1, disulfide high mobility group box 1, kynurenine pathway, neuroinflammatory cytokines

Introduction

The alarmin protein, high mobility group box-1 (HMGB1), exhibits varying biological activities depending on its location and state (1). In the nucleus, it acts as a DNA chaperone and is involved in various physiological functions, including repair, replication and transcription (2); under various stress conditions, HMGB1 is transported to the cytoplasm to contribute to immune responses and mediate autophagy (3). When released into the extracellular environment, HMGB1 exerts varying functions depending on the receptors and complexes with which it interacts (4-6). Generally, the biological activity of HMGB1 in the extracellular matrix depends on the redox state of its three cysteines (7). When the cysteines at positions C23, C45 and C106 are all reduced (in the thiol state), fully reduced HMGB1 (fr-HMGB1) is formed. In disulfide HMGB1 (ds-HMGB1), C23 and C45 form a disulfide bond with an A box in the first HMGB1 HMG-box domain, whereas C106 in the B box remains in the thiol state. The final variant, fully oxidized HMGB1 (ox-HMGB1), is reportedly non-active, with all three cysteines terminally oxidized (2,8).

Previously, Frank *et al* (9) investigated the role of the HMGB1 redox state in inflammation, and reported that ds-HMGB1, but not fr-HMGB1 contributed to inflammatory responses. Notably, as reported in our previous study, fr-HMGB1 upregulated TNF-α and induced depressive-like behavior, similar to ds-HMGB1 (4). The experimental conditions varied between the two reports; however, the mechanisms underlying the abilities of the two states, in particular fr-HMGB1, to induce depressive-like behavior merited further investigation.

The serotonin hypothesis, which suggests that low serotonin levels cause depression, was proposed in the 1960s (10-12); in subsequent decades, the role of serotonin in the pathogenesis of depression has been extensively studied. Lapin and Oxenkrug (13) hypothesized that serotonin deficiency in depression is a result of the switch of tryptophan (Trp) metabolism from serotonin synthesis to kynurenine (KYN) production. Then, the KYN pathway was revealed to be a process that starts with Trp metabolism and ends with NAD^+ production (14,15). Trp is metabolized to KYN by the rate-limiting enzyme indoleamine-2,3-dioxygenase

(IDO), which is stimulated by proinflammatory cytokines, or tryptophan-2,3-dioxygenase (TDO; Table I) (15). Subsequently, kynurenine monooxygenase (KMO) synthesizes 3-hydroxykynurenine (3-HK), which is converted into 3-hydroxyanthranilic acid (3-HANA) by kynureninase (KYNU) (14). Then, 3-HANA is oxidized by 3-hydroxyanthranilate 3,4-dioxygenase (3-HAO), resulting in quinolinic acid (QUIN) production and ultimately NAD^+ synthesis (14). Alternatively, KYN is directly converted into kynurenic acid (KYNA) by the enzyme kynurenine aminotransferase 2 (KAT2) (14).

The present study aimed to investigate the mechanisms by which HMGB1 may directly induce depressive-like behavior and determine the state in which it induces its effects.

Materials and methods

Animals and treatments. In the present study, a total of 20 8-week-old male mice (BALB/c, 22-25 g) were obtained from the Animal Center of the Second Military Medical University (Shanghai, China). Prior to experiments, mice were adapted to housing conditions (temperature, 20±1˚C; humidity, 52±2%; 12:12-h light/dark cycle; access to water and food *ad libitum*) for 2 weeks. Then, the animals were randomly assigned to the vehicle control, ds-HMGB1, fr-HMGB1 or non-oxidizable chemokine (nonoxid)-HMGB1 groups (n=5 mice/group). All procedures were conducted in accordance with the guidelines issued by the Second Military Medical University, and was approved by the Committee on Ethics of Biomedicine Research, Second Military Medical University.

Intracerebroventricular injection and sample preparation. Intracerebroventricular injections were performed as previously described (Fig. 1) (4). At 20 h after injection of HMGB1 (4 mg/ml) or vehicle (0.9% normal saline), behavioral tests were performed to evaluate depressive-like behavior. Then, mice were anesthetized with 4% chloral hydrate (400 mg/kg, intraperitoneal) and hippocampi were dissected immediately following decapitation, flash frozen in liquid nitrogen, and stored at -80˚C until subsequent use.

Behavioral tests. All behavioral tests were performed during the dark phase (07:00 p.m.-09:00 p.m.). The sucrose preference test (SPT), tail suspension test (TST) and open field test (OFT) were used as behavioral parameters to evaluate depression-like behavior as previously described (4).

Reagents. Ds-HMGB1 (cat. no. HM-122), fr-HMGB1 (cat. no. HM-116) and nonoxid-HMGB1 (cat. no. HM-132) were purchased from HMGBiotech. DMEM containing 4.5 g/l D-glucose and L-glutamine (cat. no. 11965-092) and heat inactivated horse serum (cat. no. 26050-070) were obtained from Gibco (Thermo Fisher Scientific, Inc.). Hank's balanced salt solution (HBSS; cat. no. B410) was purchased from BasalMedia.

Organotypic hippocampal slice cultures (OHSCs). Hippocampi from 7-day-old BALB/c pups (20 mice; Animal Center of the Second Military Medical University) were obtained for OHSCs as previously described (16,17). In brief, mice were sacrificed immediately upon arrival, and brains were extracted and sectioned into 400-μm transverse slices using a vibratome (ZQP-86; Shanghai Zhisun Equipment Co., Ltd.). The hippocampal slices were placed onto 0.45-μm porous membrane inserts (cat. no. FHLC 02500; EMD Millipore) and cultured in 6-well culture plates containing 1.25 ml medium (25% horse serum, 25% HBSS and 50% DMEM). Slices were maintained in an incubator (37˚C, 5% CO_2) for 7 days, with the medium replaced every 2 days. OHSCs were rinsed three times with serum-free DMEM and incubated for 2 h prior to addition of serum-free medium and treatments [80 nM HMGB1, 1 mM H_2O_2 (18)]. Fr-HMGB1 was exposed to 1 mM H_2O_2 for 1 h and dialyzed prior to treatment. Tissue and supernatant samples were collected and frozen at -80˚C for subsequent analysis following 6 h of treatment. Additionally, lactate dehydrogenase released by damaged cells was measured as a surrogate marker of tissue damage (data not shown).

Reverse transcription-quantitative PCR (RT-qPCR). Total RNA was extracted from mouse tissues and OHSCs using TRNzol-A+ reagent (cat. no. DP421; Tiangen Biotech Co., Ltd.) and reverse transcribed into cDNA using a PrimeScript™ RT Master Mix (Perfect Real Time) kit (cat. no. RR036A; Takara Bio, Inc.). RT solution was prepared on ice, and RT was performed at 37˚C for 15 min and 85˚C for 5 sec, and cDNA was stored at 4˚C. Forward and reverse primer sequences are presented in Table I. qPCR was performed using an SYBR® Premix Ex Taq™ (Tli RNaseH Plus) kit (cat. no. RR420A; Takara Bio, Inc.). The conditions of reverse transcription reaction were run in this sequence: 37˚C for 15 min, 85˚C for 5 sec, 4˚C for stored. qPCR was conducted under the following conditions: 95˚C for 30 sec, followed by 40 cycles of 95˚C for 5 sec and 60˚C for 34 sec. Experiments were performed in triplicate, and β-actin was used to normalize target gene expression following quantification of expression using the $2^{-\Delta\Delta Cq}$ method (19).

Western blot analysis. The proteins extracted from mouse hippocampi were blended in microfuge tubes with 25 mg tissue/0.25 ml RIPA buffer containing 1 mM PMSF protease inhibitor (Beyotime Institute of Biotechnology). The samples were kept on ice for 30 min and centrifuged at 10,000 x g for 5 min at 4˚C before the lysate supernatants were collected. The protein concentration was determined using a BCA Protein Assay kit (cat. no. P0010, Beyotime Institue of Biotechnology). Samples containing equal quantities of protein (20 μg) were separated via SDS-PAGE on 10% gels and transferred onto polyvinylidene fluoride membranes. The membranes were blocked by 5% nonfat dried milk in TBS-0.1% Tween-20 at room temperature for 1 h and incubated overnight at 4˚C with the following primary antibodies from ProteinTech Group, Inc.: Anti-GAPDH (1:2,000; cat. no. 10494-1-AP); anti-IDO (1:200; cat. no. 66528-1-lg); anti-KMO (1:500; cat. no. 10698-1-AP); anti-KYNU (1:1,000; cat. no. 11796-1-AP) and anti-KAT2 (1:800; cat. no. 14983-1-AP). Following incubation with the secondary antibody [IRDye-conjugated anti-rabbit (cat. no. 926-32211) and anti-mouse (cat. no. 926-68070) immunoglobulin G; 1:5,000; LI-COR Biosciences)] for 1 h at room temperature, the membranes were scanned. The integrated optical density (IOD) was calculated by use of an

Table I. Target genes analyzed via reverse transcription-quantitative PCR.

Gene name	Primer sequence (5'→3')	Function
IDO	F: GCTTTGCTCTACCACATCCAC R: CAGGCGCTGTAACCTGTGT	Oxidation, Trp→KYN
KAT2	F: ATGAATTACTCACGGTTCCTCAC R: AACATGCTCGGGTTTGGAGAT	Cleavage, KYN→KYNA
KMO	F: ATGGCATCGTCTGATACTCAGG R: CCCTAGCTTCGTACACATCAACT	Oxidation, KYN→3-HK
KYNU	F: AGTGGGCTGCACTTTTATACTG R: TGCAAACAGGTTGCCTTTCAG	Conversion, 3-HK→3-HANA
3-HAO	F: GAACGCCGTGTGAGAGTGAA R: CCAACGAACATGATTTTGAGCTG	Oxidation, 3-HANA→QUIN
β-actin	F: TTCTTGGGTATGGAATCCTGT R: AGCACTGTGTTGGCATAGAG	Cytoskeleton

F, forward; R, reverse; IDO, indoleamine-2,3-dioxygenase; KAT2, kynurenine aminotransferase 2; KMO, kynurenine monooxygenase; KYN, kynurenine; KYNA, kynurenic acid; KYNU, kynureninase; Trp, tryptophan; 3-HAO, 3-hydroxyanthranilate 3,4-dioxygenase; 3-HANA, 3-hydroxyanthranilic acid; 3-HK, 3-hydroxykynurenine.

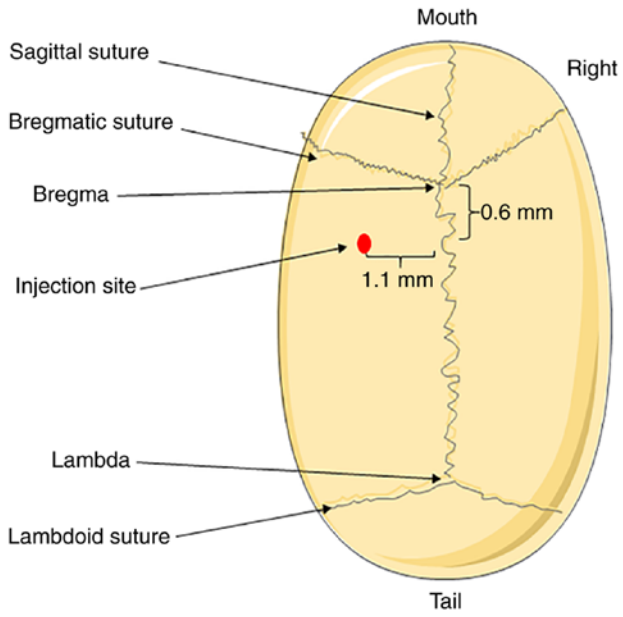

Figure 1. Coordinates of intracerebral ventricular injection. The cannula tip was placed at the following stereotaxic coordinates: Anteroposterior: -0.6 mm; mediolateral: -1.1 mm; dorsoventral: -2 mm.

Odyssey Infrared Imaging System (LI-COR Biosciences) and ImageJ software (1.48v; National Institutes of Health).

ELISA. The concentrations of tumor necrosis factor-α (TNF-α; cat. no. F11630) and interleukin-1β (IL-1β; cat. no. F10770) in the OHSC supernatant were detected using corresponding ELISA kits according to the manufacturer's protocols (Westang, Inc.). Briefly, 100 μl of each sample was added to ELISA plates in duplicate. The lower limits of detection were 4 pg/ml for TNF-α and 8 pg/ml for IL-1β. The absorbance was measured on a microplate reader (Synergy™ H1; BioTek Instruments, Inc.).

Total reactive oxygen species (ROS) measurement. Hippocampal ROS levels were measured in hippocampal lysates using the OxiSelect™ *In Vitro* ROS/RNS Assay kit from Cell Biolabs, Inc. (cat. no. STA-347). The samples and standards (hydrogen peroxide) were mixed with fluorogenic stabilized dichlorodihydrofluorescein (DCF) and incubated at room temperature for 30 min. In the presence of ROS, DCF was oxidized and the fluorescence was detected (excitation 480 nm/emission 530 nm).

Following the completion of all behavioral tests, mice were intraperitoneally anesthetized using 4% chloral hydrate (400 mg/kg, intraperitoneal administration) and perfused transcardially with 0.9% saline followed by ice-cold 4% paraformaldehyde (PFA; cat. no. G1101; Wuhan Servicebio Technology Co., Ltd.). Following fixation for 4-8 h fix in 4% PFA, brains were dehydrated in 20% sucrose for 2-3 days. The brains were then embedded in paraffin and sectioned (4 μm). Prior to assays, sections were deparaffinized in xylene and rehydrated in a graded ethanol series. In brief, slices were incubated with 20 μM dihydroethidium (DHE; cat. no. D7008; Sigma-Aldrich; Merck KGaA) for 30 min at 37˚C, followed by incubation with DAPI (1:1,000; cat. no. D9542; Sigma-Aldrich; Merck KGaA) for 10 min at room temperature. Images were obtained using a fluorescence microscope (magnification, x200; Carl Zeiss AG) at an excitation wavelength of 370 nm and emission wavelength of 420 nm.

Statistical analysis. GraphPad Prism 6.01 (GraphPad Software, Inc.) was used for data analysis. Two-way ANOVA with post hoc Tukey's multiple comparison test was performed to evaluate the main effects and interactions of fr-HMGB1 and H_2O_2 *in vivo*. One-way ANOVA followed by Tukey's multiple comparison test was used to analyze the effects of fr-HMGB1 and ds-HMGB1 *in vivo* and *in vitro*. The Mann-Whitney test was performed to compare ROS levels in the control and fr-HMGB1 groups. Data are presented as the mean ± standard

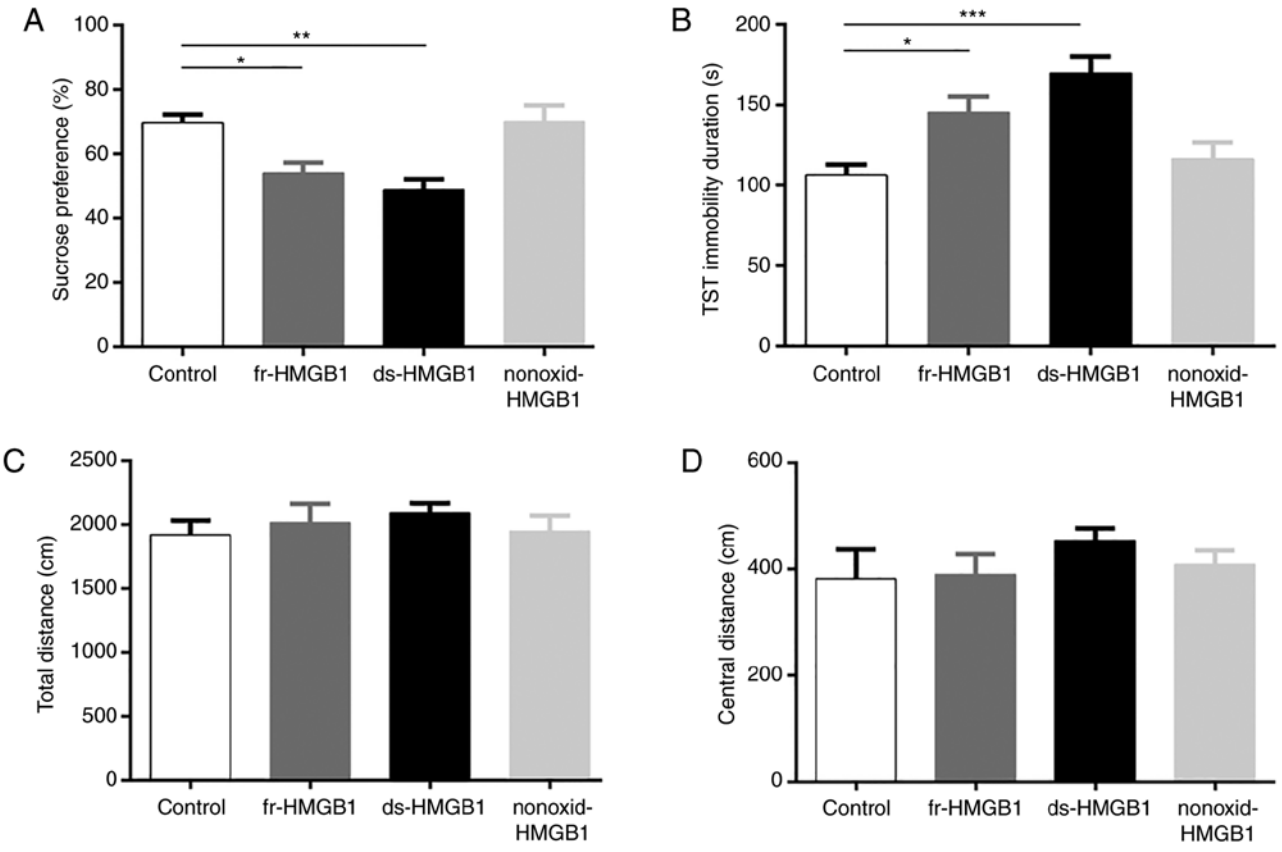

Figure 2. HMGB1 at different redox states induces distinct effects on the development of depressive-like behavior in mice. Effects of fr-, ds- and nonoxid-HMGB1 on (A) sucrose preference and (B) duration of immobility in the TST. Effects of HMBG1 on (C) total distance and (D) central distance traveled in the open field test. Data are presented as the mean ± SEM (n=5/group). *P<0.05, **P<0.01, ***P<0.001. ds-, disulfide; fr-, fully reduced; HMGB1, high mobility group box-1; nonoxid-, non-oxidizable chemokine; TST, tail suspension test.

error of the mean. Each experiment was repeated three times. P<0.05 was considered to indicate a statistically significant difference.

Results

Central administration of fr- and ds-HMGB1, but not nonoxid-HMGB1, induces depressive-like behavior. Several behavioral tests were conducted to evaluate the depressive-like behavior of mice following administration of recombinant HMGB1, including fr-HMGB1, ds-HMGB1 and nonoxid-HMGB1. Nonoxid-HMGB1, in which all cysteines are replaced by serine residues, is a mutant analogue of fr-HMGB1 (18). The TST was used to evaluate antidepressant activity (20) in experimental animals. In the SPT, low intake of sucrose solution is hypothesized to indicate anhedonia and impaired sensitivity to reward (21). The total distance travelled during the can be affected by a number of factors, including an animal's sickness behavior (22), and its anxiety status can be assayed from the central distance covered (22).

Sucrose preference was significantly decreased following injection of fr- (P<0.05) and ds-HMGB1 (P<0.01) compared with control treatment (F=8.665, P=0.0012; Fig. 2A). Additionally, the duration of immobility in the TST (F=9.749, P=0.0007; Fig. 2B) was strongly significantly increased following ds-HMGB1 (P<0.001) administration, and significantly increased in fr-HMGB1-treated (P<0.05) mice compared with the control group. Conversely, nonoxid-HMGB1 did not significantly affect sucrose preference (Fig. 2A) or increase immobility duration (Fig. 2B). In addition, there were no significant differences in total (Fig. 2C) and central distance travelled in the OFT (Fig. 2D) between groups. The results indicated that the fr- and ds-HMGB1-treated animals exhibited depressive-like behavior without a notable anxiety or sickness phenotype, consistent with our previous study (4). Based on these findings, the molecular mechanisms and role of HMGB1 in mouse models were further studied.

Administration of fr-HMGB1 and ds-HMGB1 upregulates the expression of the enzymes of the KYN pathway in vivo, whereas nonoxid-HMGB1 induces no effects. As described, ds-HMGB1 and fr-HMGB1 contributed to depressive-like behavior, whereas nonoxid-HMGB1 did not. The mRNA expression and relative protein levels of essential KYN pathway enzymes in the hippocampus were analyzed following intracerebroventricular administration of various HMGB1 forms.

As presented in Fig. 3A, IDO (F=8.630, P=0.0008) was upregulated in ds-HMGB1-(P=0.0132) and fr-HMGB1-treated (P<0.01) hippocampi compared with the control group. Similar results were obtained for KMO (F=5.955, P=0.0049; Fig. 3A) and KYNU (F=7.114, P=0.0019; Fig. 3A) after ds-HMGB1 administration. Notably, fr-HMGB1 treatment significantly increased KMO (P<0.05; Fig. 3A) and KYNU

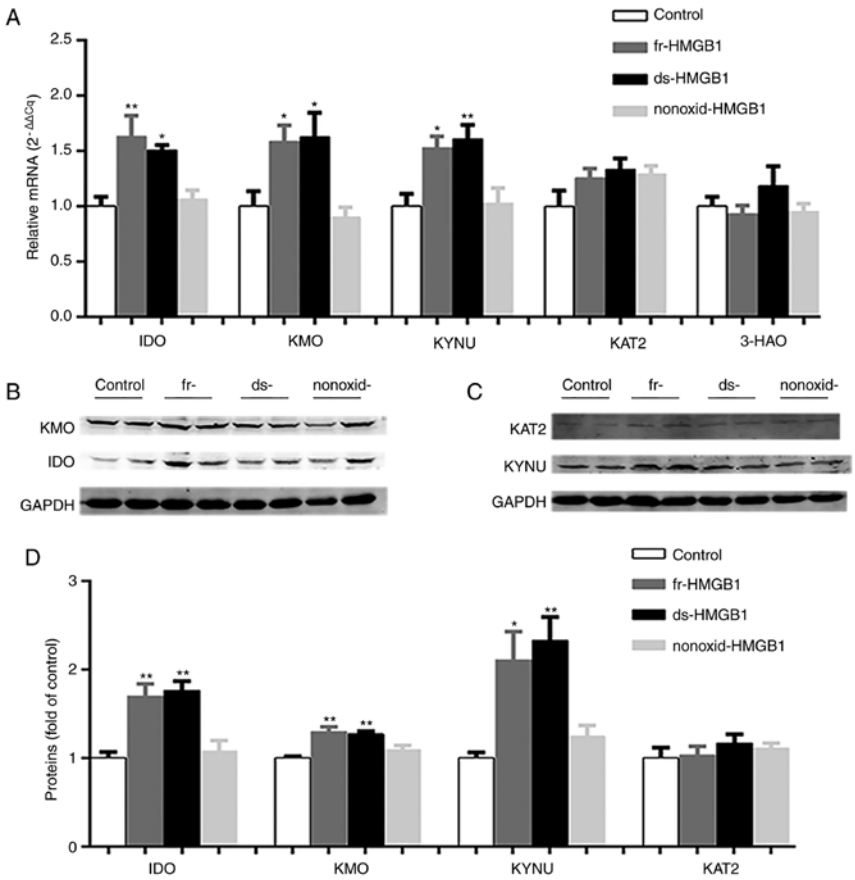

Figure 3. Expression levels of enzymes in the kynurenine pathway are increased in fr-HMGB1 and ds-HMGB1-treated mice. (A) Gene expression levels of IDO, KMO, KYNU, KAT2 and 3-HAO relative to control samples, as determined via reverse transcription-quantitative PCR analysis. Representative western blots of the protein levels of (B) IDO and KMO, (C) KAT2 and KYNU in hippocampi. (D) Semi-quantification of protein expression. Data are presented as the mean ± SEM (n=5/group). *P<0.05, **P<0.01. ds-, disulfide; fr-, fully reduced; HMGB1, high mobility group box-1; IDO, indoleamine-2,3-dioxygenase; KAT2, kynurenine aminotransferase 2; KMO, kynurenine monooxygenase; KYNU, kynureninase; nonoxid-, non-oxidizable chemokine; 3-HAO, 3-hydroxyanthranilate 3,4-dioxygenase.

(P=0.0161; Fig. 3A) gene expression levels compared with the vehicle group, suggesting that ds-HMGB1 and fr-HMGB1 each activated the KYN pathway *in vivo*. Conversely, central administration of nonoxid-HMGB1 did not significantly affect IDO, KMO and KYNU mRNA levels (Fig. 3A). Treatment with the three HMGB1 did not significantly alter 3-HAO and KAT2 expression levels compared with the control group (Fig. 3A).

In addition to detecting the mRNA expression of KYN pathway-associated enzymes, their relative protein expression was also determined. As presented in Fig. 3B-D, ds- and fr-HMGB1 treatment significantly upregulated the hippocampal expression of IDO (F=13.16, P=0.0004), KMO (F=12.1, P=0.0006) and KYNU (F=8.9, P=0.0022) proteins compared with the control group; conversely, there was no significant difference in the protein levels of KAT2 (Fig. 3C and D) between four groups. In addition, no significant effects were identified for nonoxid-HMGB1 treatment in those four enzymes (Fig. 3B-D). The altered expression of KYN pathway enzymes in mice following administration of different forms of HMGB1, combined with HMGB1 central administration-induced depressive-like behavior (Fig. 2A-D), further indicated the molecular mechanisms underlying the effects of different forms of HMGB1 in relation to depression.

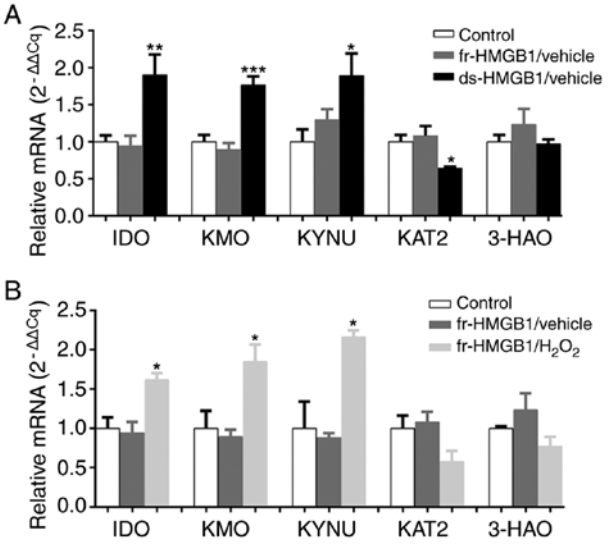

Figure 4. Oxidized fr-HMGB1 induces the kynurenine pathway in cultured hippocampus slices. Gene expression levels of IDO, KMO, KYNU, KAT2 and 3-HAO in OHSCs treated with (A) fr- and ds-HMGB1, and (B) fr-HMGB1 and H_2O_2, as determined via reverse transcription-quantitative PCR analysis. Data are presented as the mean ± SEM (n=3-5/group). *P<0.05, **P<0.01, ***P<0.001 vs. Control. ds-, disulfide; fr-, fully reduced; HMGB1, high mobility group box-1; IDO, indoleamine-2,3-dioxygenase; KAT2, kynurenine aminotransferase 2; KMO, kynurenine monooxygenase; KYNU, kynureninase; 3-HAO, 3-hydroxyanthranilate 3,4-dioxygenase.

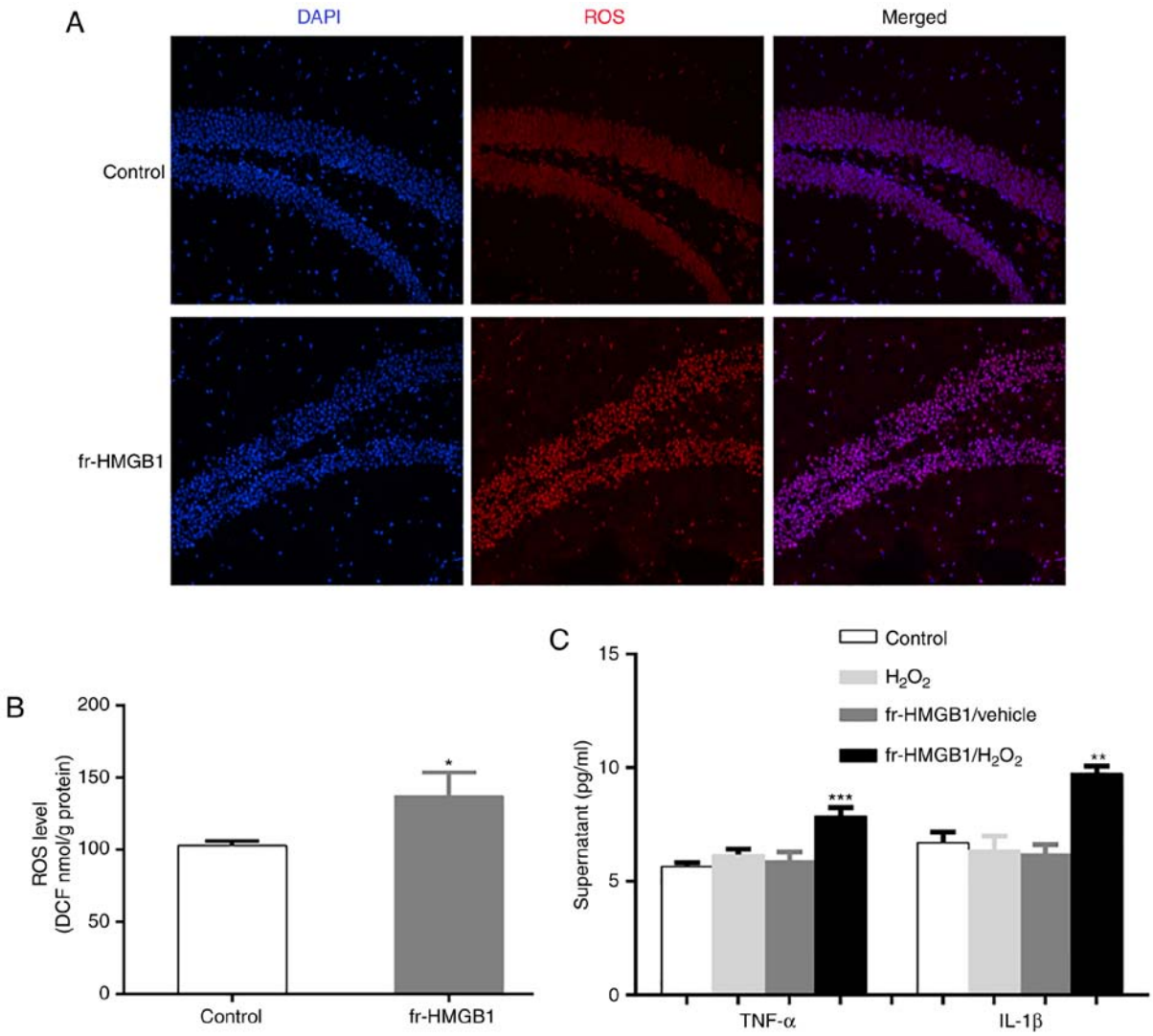

Figure 5. TNF-α and IL-1β levels in tissue slices and ROS production in the hippocampus. (A and B) ROS levels in the hippocampus, as determined in brain slices by dihydroethidium fluorescence and in hippocampal lysates by DCF fluorescence. (C) Following the treatment of organotypic hippocampal slice cultures for 6 h with fr-HMGB1 and H_2O_2, supernatants were collected and tested for TNF-α and IL-1β protein levels. Data are presented as the mean ± SEM (n=3-5/group). *P<0.05, **P<0.01, ***P<0.001 vs. Control. DCF, dichlorodihydrofluorescein; fr-, fully reduced; HMGB1, high mobility group box-1; IL-1β, interleukin-1β; TNF-α, tumor necrosis factor-α.

Following oxidation by H_2O_2, fr-HMGB1 activates the enzymes of the KYN pathway in cultured hippocampus slices. To further investigate the varied effects of fr- and ds-HMGB1 on the KYN pathway, essential proteins of the KYN pathway were evaluated following treatment of OHSCs with fr- and ds-HMGB1 *in vitro*. There were no significant differences in IDO, KMO, KYNU and KAT2 expression levels between the control and fr-HMGB1 groups (Fig. 4A). Consistent with the results of central ds-HMGB1 administration, the expression levels of IDO (F=10.07, P=0.0033), KMO (F=17.88, P=0.0003) and KYNU (F=4.779, P=0.0321) were increased in tissue slices following ds-HMGB1 administration compared with the control group (Fig. 4A). Notably, KAT2 mRNA gene expression was decreased in the ds-HMGB1 treatment group (F=5.082, P=0.0273; Fig. 4A), in contrast to the *in vivo* experiments. In addition, ds- and fr-HMGB1 did not significantly alter 3-HAO expression compared with the control group (Fig. 4A). These results indicated that ds-HMGB1 administration, but not fr-HMGB1, activated the KYN pathway *in vitro*.

To determine the mechanism by which fr-HMGB1 induces the KYN pathway *in vivo* but not *in vitro*, the expression of KYN pathway effectors in OHSCs was evaluated following treatment with various combinations of fr-HMGB1 and H_2O_2. As presented in Fig. 4B, one-way ANOVA demonstrated significant differences between the three groups (P=0.0153, F=9.078). Multiple comparisons indicated that exposure for 6 h to fr-HMGB1 + H_2O_2 resulted in significantly increased IDO expression (P<0.05). In addition to IDO, other essential enzymes (KMO, KYNU, 3-HAO and KAT2) involved in the metabolism of KYN along the KYN pathway were analyzed via RT-qPCR. No effects on KMO, KYNU, KAT2 and 3-HAO expression levels were observed following fr-HMGB1 treatment compared with the control group (Fig. 4B); however, following oxidation by H_2O_2, fr-HMGB1 significantly increased the gene expression levels of KMO (F=7.841, P=0.0212; Fig. 4B) and KYNU (F=11.99, P=0.008; Fig. 4B) in tissue slices. Combined with the aforementioned results, these findings suggested that fr-HMGB1 activated the KYN pathway indirectly following oxidation.

Effects of fr-HMGB1 on neuroinflammatory cytokines in vitro and ROS production in the brain. It has been reported that central inflammatory cytokine levels are increased during the development of depressive-like behavior (23,24). Therefore, TNF-α and IL-1β levels in OHSC supernatants following treatment with fr-HMGB1, in presence or absence of its oxidant, were detected by ELISA. As presented in Fig. 5C, there were significant fr-HMGB1 x H_2O_2 interactions for secreted TNF-α (F=4.793, P=0.039) and IL-1β (F=16.45, P=0.0006) protein levels. Fr-HMGB1 treatment did not increase the levels of TNF-α and IL-1β in control slices; however, combination with H_2O_2 treatment increased cytokine levels (TNF-α, P<0.001; IL-1β, P<0.001; Fig. 5C). These findings indicated that fr-HMGB1 activated TNF-α and IL-1β signaling only following oxidation. In addition, hippocampal ROS levels were significantly increased in the fr-HMGB1 group compared with the control group (P<0.05; Fig. 5A and B), as measured by DHE and DCF fluorescence.

Discussion

Consistent with our previous study (4), the findings of the present study demonstrated that i) both states of HMGB1 induced the KYN pathway, resulting in depressive-like behavior; ii) KYN pathway activation occurred via similar mechanisms, with ds-HMGB1 directly upregulating KYN pathway enzymes (IDO, KMO and KYNU), and fr-HMGB1 upregulating expression only following oxidation to ds-HMGB1.

As aforementioned, HMGB1 exists in three different forms. Its biological activities rely on these forms, which vary based on the oxidation states of cysteine residues at C23, C45 and C106 (18,25). Ds-HMGB1 acts as a proinflammatory cytokine by binding to toll-like receptors (7,25), whereas fr-HMGB1 mediates chemotaxis via interactions with receptor for advanced glycation end products (18). Conversely, ox-HMGB1 has no known active function. Consistent with our previous study (4), the present study demonstrated that ds-HMGB1 induced the activation of the KYN pathway and other proinflammatory cytokines *in vivo* and *ex vivo*, thus verifying the possible etiology of ds-HMGB1-induced depression.

Of note, fr-HMGB1 also induced the KYN pathway, upregulating cytokines such as TNF-α *in vivo* (4), and contributing to the development of depressive behavior. Conversely, it did not upregulate the KYN pathway or increase TNF-α and IL-1β levels *ex vivo* unless in presence of the oxidant H_2O_2. Furthermore, the mutant analogue of fr-HMGB1, nonoxid-HMGB1, which exhibits chemoattractant activity but lacks oxidizable activity (18), did not induce depressive-like behavior or KYN pathway activation. This difference between the two states of HMGB1 is proposed to result from the fact that nonoxid-HMGB1 cannot be oxidized into ds-HMGB1, whereas extracellular fr-HMGB1 is able to alter its state from a reduced to oxidized form *in vivo* (25). Overall, combined with *ex vivo* findings, it is proposed that fr-HMGB1 may contribute to depression following oxidation *in vivo*. Additionally, the levels of ROS were increased following central administration of fr-HMGB1, supporting the aforementioned hypothesis. Increased ROS levels suggested that the extracellular milieu may be more oxidizing, enabling the formation of disulfide bridges (26).

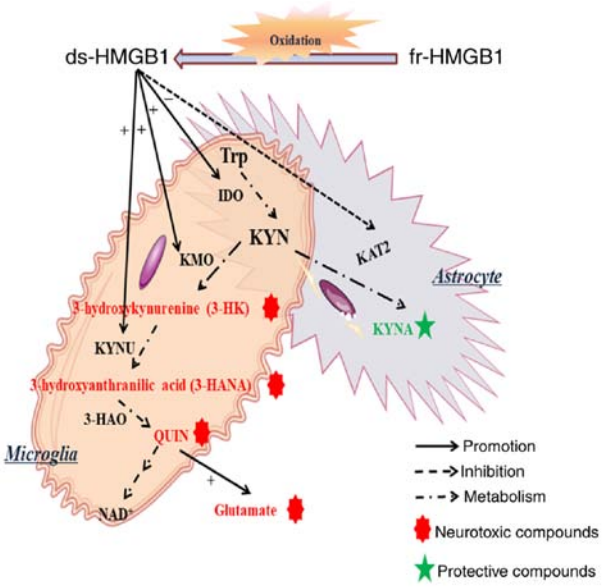

Figure 6. Model of fr- and ds-HMGB1-mediated neurotoxicity. Ds-HMGB1 upregulated the expression of certain enzymes associated with the kynurenine pathway mainly located in microglia but not in astrocytes; fr-HMGB1 induced similar effects following oxidation. It was hypothesized that the disbalance of the two kynurenine pathway arms in the brain reinforced neurotoxic metabolite neurotransmission, inhibited the production of neuroprotective compounds and contributed to the occurrence of depression. ds-, disulfide; fr-, fully reduced; HMGB1, high mobility group box-1; IDO, indoleamine-2,3-dioxygenase; KAT2, kynurenine aminotransferase 2; KMO, kynurenine monooxygenase; KYN, kynurenine; KYNA, kynurenic acid; KYNU, kynureninase; 3-HAO, 3-hydroxyanthranilate 3,4-dioxygenase; Trp, tryptophan.

The present study revealed that ds-HMGB1 and fr-HMGB1 activated the KYN pathway. As aforementioned, Trp metabolism by IDO or TDO2 is the first step of the KYN pathway; when Trp is converted into KYN, it can be metabolized by KMO, KYUN and 3-HAO to yield 3-HK, QUIN and NAD^+; alternatively, it can be converted into KYNA by KAT2. Of note, KYN derivatives in the Trp-NAD^+ pathway include neurotoxic compounds such as 3-HK and QUIN (14), unlike the protective product KYNA synthesized by KAT2. The increased expression levels of IDO, KMO and KYNU, but not KAT2 suggested that fr-HMGN1 and ds-HMGB1 induced the Trp-NAD^+ pathway, but not the Trp-KYNA axis (Fig. 6). KYNU is detected in microglia (27), whereas KAT2 is produced by astrocytes (28,29). These findings suggested the involvement of microglial (but not astrocytic) activation. Subsequently, activated microglia may secrete abundant glutamate (Fig. 6), which is also considered to be neurotoxic (30), and uptake KYN (14). Thus, the Trp-NAD^+ pathway in microglia requires further investigation. Of note, differences in KAT2 expression in response to HMBG1 treatment were observed between whole hippocampi and slice cultures; KAT2 exhibited a trend towards upregulated expression *in vivo* but was downregulated *in vitro*, suggesting that extrahippocampal regions may serve protective functions; however, this requires further investigation.

The effects of HMGB1 have been reported in numerous diseases, including sepsis, arthritis and ischemia-reperfusion,

with the application of HMGB1-blocking therapies improving symptoms in rodent models of these disorders (31-33); certain studies focused on ds-HMGB1 (6,9,34). In the present study, it was demonstrated that an oxidative environment *in vivo* and *ex vivo* may oxidize fr-HMGB1, conferring ds-HMGB1 characteristics and mediating depression via the KYN pathway.

The present study investigated the role of fr-HMGB1 in the induction KYN pathway; however, the role of other mechanisms cannot be excluded. Additionally, the effects of systemic ROS depletion using antioxidant compounds or vitamins supplements, and the measurement of antioxidant enzyme levels or KYN pathway metabolites *in vivo* or *in vitro* require investigation. Overall, further study is required to determine the precise mechanisms and effects of fr-HMGB1.

Acknowledgements

The authors would like to thank Dr Huang Xiao (Institute of Neuroscience and Key Laboratory of Molecular Neurobiology of Ministry of Education, Second Military Medical University, Shanghai, China) for technical assistance and editing of the manuscript.

Funding

The present study was financially supported by the National Natural Science Foundation of China (grant nos. 81171124 and 81771301).

Availability of data and materials

The datasets used and/or analyzed during the current study are available from the corresponding author on reasonable request.

Authors' contributions

BW drafted the manuscript and contributed to all aspects of the experimental design and research procedure, including western blotting and qPCR assays. YJL was involved in conducting the behavioral measurements. LLL and JML contributed to conducting the experiments. WJS and CLJ made substantial contributions to the conception of the study and the editing of the manuscript. YXW was involved in designing the study and interpreting the data. All authors read and approved the final manuscript.

Ethics approval and consent to participate

The present study was approved by the Committee on Ethics of Biomedicine Research, Second Military Medical University and conducted in accordance with the guidelines of Animal Experimentation set by the committee.

Patient consent for publication

Not applicable.

Competing interests

The authors declare that they have no competing interests.

References

1. Magna M and Pisetsky DS: The role of HMGB1 in the pathogenesis of inflammatory and autoimmune diseases. Mol Med 20: 138-146, 2014.
2. Kang R, Chen R, Zhang Q, Hou W, Wu S, Cao L, Huang J, Yu Y, Fan XG, Yan Z, *et al*: HMGB1 in health and disease. Mol Aspects Med 40: 1-116, 2014.
3. Avgousti DC, Herrmann C, Kulej K, Pancholi NJ, Sekulic N, Petrescu J, Molden RC, Blumenthal D, Paris AJ, Reyes ED, *et al*: A core viral protein binds host nucleosomes to sequester immune danger signals. Nature 535: 173-177, 2016.
4. Lian YJ, Gong H, Wu TY, Su WJ, Zhang Y, Yang YY, Peng W, Zhang T, Zhou JR, Jiang CL and Wang YX: Ds-HMGB1 and fr-HMGB induce depressive behavior through neuroinflammation in contrast to nonoxid-HMGB1. Brain Behav Immun 59: 322-332, 2017.
5. Balosso S, Liu J, Bianchi ME and Vezzani A: Disulfide-containing high mobility group box-1 promotes N-methyl-D-aspartate receptor function and excitotoxicity by activating Toll-like receptor 4-dependent signaling in hippocampal neurons. Antioxid Redox Signal 21: 1726-1740, 2014.
6. Mazarati A, Maroso M, Iori V, Vezzani A and Carli M: High-mobility group box-1 impairs memory in mice through both toll-like receptor 4 and receptor for advanced glycation end products. Exp Neurol 232: 143-148, 2011.
7. Frank MG, Weber MD, Watkins LR and Maier SF: Stress sounds the alarmin: The role of the danger-associated molecular pattern HMGB1 in stress-induced neuroinflammatory priming. Brain Behav Immun 48: 1-7, 2015.
8. Yang H, Antoine DJ, Andersson U and Tracey KJ: The many faces of HMGB1: Molecular structure-functional activity in inflammation, apoptosis, and chemotaxis. J Leukoc Biol 93: 865-873, 2013.
9. Frank MG, Weber MD, Fonken LK, Hershman SA, Watkins LR and Maier SF: The redox state of the alarmin HMGB1 is a pivotal factor in neuroinflammatory and microglial priming: A role for the NLRP3 inflammasome. Brain Behav Immun 55: 215-224, 2016.
10. Coppen AJ: Depressed states and indolealkylamines. Adv Pharmacol 6: 283-291, 1968.
11. Carlsson A, Corrodi H, Fuxe K and Hökfelt T: Effect of antidepressant drugs on the depletion of intraneuronal brain 5-hydroxytryptamine stores caused by 4-methyl-alpha-ethyl-meta-tyramine. Eur J Pharmacol 5: 357-366, 1969.
12. Schildkraut JJ: The catecholamine hypothesis of affective disorders: A review of supporting evidence. Am J Psychiatry 122: 509-522, 1965.
13. Lapin IP and Oxenkrug GF: Intensification of the central serotoninergic processes as a possible determinant of the thymoleptic effect. Lancet 1: 132-136, 1969.
14. Maddison DC and Giorgini F: The kynurenine pathway and neurodegenerative disease. Semin Cell Dev Biol 40: 134-141, 2015.
15. Dantzer R, O'Connor JC, Lawson MA and Kelley KW: Inflammation-associated depression: From serotonin to kynurenine. Psychoneuroendocrinology 36: 426-436, 2011.
16. Brooks AK, Lawson MA, Smith RA, Janda TM, Kelley KW and McCusker RH: Interactions between inflammatory mediators and corticosteroids regulate transcription of genes within the Kynurenine Pathway in the mouse hippocampus. J Neuroinflammation 13: 98, 2016.
17. Wang B, Lian YJ, Su WJ, Peng W, Dong X, Liu LL, Gong H, Zhang T, Jiang CL and Wang YX: HMGB1 mediates depressive behavior induced by chronic stress through activating the kynurenine pathway. Brain Behav Immun 72: 51-60, 2018.
18. Venereau E, Casalgrandi M, Schiraldi M, Antoine DJ, Cattaneo A, De Marchis F, Liu J, Antonelli A, Preti A, Raeli L, *et al*: Mutually exclusive redox forms of HMGB1 promote cell recruitment or proinflammatory cytokine release. J Exp Med 209: 1519-1528, 2012.
19. Livak KJ and Schmittgen TD: Analysis of relative gene expression data using real-time quantitative PCR and the 2(-Delta Delta C(T)) method. Methods 25: 402-408, 2001.
20. Cryan JF, Mombereau C and Vassout A: The tail suspension test as a model for assessing antidepressant activity: Review of pharmacological and genetic studies in mice. Neurosci Biobehav Rev 29: 571-625, 2005.

21. Liu MY, Yin CY, Zhu LJ, Zhu XH, Xu C, Luo CX, Chen H, Zhu DY and Zhou Q: Sucrose preference test for measurement of stress-induced anhedonia in mice. Nat Protoc 13: 1686-1698, 2018.
22. Seibenhener ML and Wooten MC: Use of the open field maze to measure locomotor and anxiety-like behavior in mice. J Vis Exp: e52434, 2015.
23. Liu YN, Peng YL, Liu L, Wu TY, Zhang Y, Lian YJ, Yang YY, Kelley KW, Jiang CL and Wang YX: TNFα mediates stress-induced depression by upregulating indoleamine 2,3-dioxygenase in a mouse model of unpredictable chronic mild stress. Eur Cytokine Netw 26: 15-25, 2015.
24. Zhang Y, Liu L, Liu YZ, Shen XL, Wu TY, Zhang T, Wang W, Wang YX and Jiang CL: NLRP3 inflammasome mediates chronic mild stress-induced depression in mice via neuroinflammation. Int J Neuropsychopharmacol 18: pii: pyv006, 2015.
25. Yang H, Lundbäck P, Ottosson L, Erlandsson-Harris H, Venereau E, Bianchi ME, Al-Abed Y, Andersson U, Tracey KJ and Antoine DJ: Redox modification of cysteine residues regulates the cytokine activity of high mobility group box-1 (HMGB1). Mol Med 18: 250-259, 2012.
26. Tang D, Kang R, Zeh HJ III and Lotze MT: High-mobility group box 1, oxidative stress, and disease. Antioxid Redox Signal 14: 1315-1335, 2011.
27. Guillemin GJ, Smith DG, Smythe GA, Armati PJ and Brew BJ: Expression of the kynurenine pathway enzymes in human microglia and macrophages. Adv Exp Med Biol 527: 105-112, 2003.
28. Schwarcz R and Pellicciari R: Manipulation of brain kynurenines: Glial targets, neuronal effects, and clinical opportunities. J Pharmacol Exp Ther 303: 1-10, 2002.
29. Du F, Schmidt W, Okuno E, Kido R, Köhler C and Schwarcz R: Localization of kynurenine aminotransferase immunoreactivity in the rat hippocampus. J Comp Neurol 321: 477-487, 1992.
30. Piani D, Spranger M, Frei K, Schaffner A and Fontana A: Macrophage-induced cytotoxicity of N-methyl-D-aspartate receptor positive neurons involves excitatory amino acids rather than reactive oxygen intermediates and cytokines. Eur J Immunol 22: 2429-2436, 1992.
31. Goldstein RS, Gallowitsch-Puerta M, Yang L, Rosas-Ballina M, Huston JM, Czura CJ, Lee DC, Ward MF, Bruchfeld AN, Wang H, *et al*: Elevated high-mobility group box 1 levels in patients with cerebral and myocardial ischemia. Shock 25: 571-574, 2006.
32. Kokkola R, Li J, Sundberg E, Aveberger AC, Palmblad K, Yang H, Tracey KJ, Andersson U and Harris HE: Successful treatment of collagen-induced arthritis in mice and rats by targeting extracellular high mobility group box chromosomal protein 1 activity. Arthritis Rheum 48: 2052-2058, 2003.
33. Zhao H, Liu Z, Shen H, Jin S and Zhang S: Glycyrrhizic acid pretreatment prevents sepsis-induced acute kidney injury via suppressing inflammation, apoptosis and oxidative stress. Eur J Pharmacol 781: 92-99, 2016.
34. Lee G, Espirito Santo AI, Zwingenberger S, Cai L, Vogl T, Feldmann M, Horwood NJ, Chan JK and Nanchahal J: Fully reduced HMGB1 accelerates the regeneration of multiple tissues by transitioning stem cells to G_{Alert}. Proc Natl Acad Sci USA 115: E4463-E4472, 2018.